

1 **A multi-task convolutional deep learning method for HLA allelic imputation**  
2 **and its application to trans-ethnic MHC fine-mapping of type 1 diabetes.**

3

4 Tatsuhiko Naito<sup>1,2</sup>, Ken Suzuki<sup>1</sup>, Jun Hirata<sup>1,3</sup>, Yoichiro Kamatani<sup>4</sup>, Koichi Matsuda<sup>5</sup>, Tatsushi  
5 Toda<sup>2</sup>, Yukinori Okada<sup>1,6,7\*</sup>.

6

7 1) Department of Statistical Genetics, Osaka University Graduate School of Medicine,  
8 565-0871, Suita, Japan.

9 2) Department of Neurology, Graduate School of Medicine, The University of Tokyo, 113-8655,  
10 Tokyo, Japan.

11 3) Pharmaceutical Discovery Research Laboratories, Teijin Pharma Limited, 191-8512, Hino,  
12 Japan

13 4) Laboratory of Complex Trait Genomics, Department of Computational Biology and Medical  
14 Sciences, Graduate School of Frontier Sciences, The University of Tokyo, 108-8639, Tokyo,  
15 Japan

16 5) Laboratory of Clinical Genome Sequencing, Department of Computational Biology and  
17 Medical Sciences, Graduate School of Frontier Sciences, The University of Tokyo,  
18 108-8639, Tokyo, Japan.

19 6) Laboratory of Statistical Immunology, Immunology Frontier Research Center (WPI-IFReC),  
20 Osaka University, 565-0871, Suita, Japan.

21 7) Integrated Frontier Research for Medical Science Division, Institute for Open and  
22 Transdisciplinary Research Initiatives, Osaka University, 565-0871, Suita, Japan.

23

24 \* Corresponding author:

25 Yukinori Okada, MD, PhD

26 Address: Department of Statistical Genetics, Osaka University Graduate School of Medicine,

27 2-2 Yamadaoka, Suita, Osaka 565-0871, Japan.

28 Tel: +81-6-6879-3971

29 E-mail: [yokada@sg.med.osaka-u.ac.jp](mailto:yokada@sg.med.osaka-u.ac.jp)

30

31 **Abstract**

32 Conventional HLA imputation methods drop their performance for infrequent alleles, which  
33 reduces reliability of trans-ethnic MHC fine-mapping due to inter-ethnic heterogeneity in allele  
34 frequency spectra. We developed DEEP\*HLA, a deep learning method for imputing HLA  
35 genotypes. Through validation using the Japanese and European HLA reference panels ( $n =$   
36 1,118 and 5,112), DEEP\*HLA achieved the highest accuracies in both datasets (0.987 and  
37 0.976) especially for low-frequency and rare alleles. DEEP\*HLA was less dependent of  
38 distance-dependent linkage disequilibrium decay of the target alleles and might capture the  
39 complicated region-wide information. We applied DEEP\*HLA to type 1 diabetes GWAS data of  
40 BioBank Japan ( $n = 62,387$ ) and UK Biobank ( $n = 356,855$ ), and successfully disentangled  
41 independently associated class I and II HLA variants with shared risk between diverse  
42 populations (the top signal at HLA-DR $\beta$ 1 amino acid position 71;  $P = 6.2 \times 10^{-119}$ ). Our study  
43 illustrates a value of deep learning in genotype imputation and trans-ethnic MHC fine-mapping.

44

45

46 **Introduction**

47 Genetic variants of the major histocompatibility complex (MHC) region at 6p21.3 contribute to  
48 the genetic of a wide range of human complex traits.<sup>1</sup> Among the genes densely contained in  
49 the MHC region, human leukocyte antigen (HLA) genes are considered to explain most of the  
50 genetic risk of MHC.<sup>1</sup> Strategies for direct typing of HLA alleles, including sequence specific  
51 oligonucleotide (SSO) hybridization, Sanger sequencing, and next-generation sequencing, do  
52 not easily scale for large cohorts since they are labor-intensive, time-consuming, expensive,  
53 and limited in terms of allele resolution and HLA gene coverage.<sup>2,3</sup> As a result, in many cases,  
54 the genotypes of HLA allele are indirectly imputed from single nucleotide variant (SNV)-level  
55 data using population-specific HLA reference panels.<sup>3-6</sup>

56 The MHC region harbors unusually complex sequence variations and haplotypes that  
57 are specific to individual ancestral populations; thus, the distribution and frequencies of the HLA  
58 alleles are highly variable across different ethnic groups.<sup>1,7</sup> This causes heterogeneity in  
59 reported HLA risk alleles of human complex diseases across diverse populations.<sup>8</sup> For example,  
60 in type I diabetes (T1D), the strong association between non-Asp57 in HLA-DQ $\beta$ 1 and T1D risk  
61 has been found in Europeans<sup>9,10</sup> but not in the Japanese population, where the T1D susceptible  
62 HLA-DQ $\beta$ 1 alleles carry Asp57.<sup>11</sup> Although elucidation of risk alleles beyond ethnicities would  
63 contribute to further understanding of genetic architecture of the MHC region associated with  
64 pathologies of complex diseases, few trans-ethnic MHC fine-mappings have been reported  
65 yet.<sup>12</sup> One of the ways of conducting trans-ethnic fine-mapping in the comprehensive MHC  
66 region is to newly construct a large HLA reference panel which captures the complexities of the  
67 MHC region across different populations.<sup>13</sup> The other is to integrate data of different populations  
68 which are imputed with a reference panel specific for each population. Although the latter way

69 seems straightforward, we need an HLA imputation method accurate enough for infrequent  
70 alleles to robustly evaluate HLA variants which are highly heterogenous in allele frequency  
71 across ethnicities.

72 Various methods for HLA allelic imputation have been developed. SNP2HLA is one of  
73 the standard software, which uses the imputation software package Beagle to impute both HLA  
74 alleles and the amino acid polymorphisms for those classical alleles.<sup>14</sup> HLA Genotype  
75 Imputation with Attribute Bagging (HIBAG)<sup>15</sup> is also promising software, which employs multiple  
76 expectation-maximization-based classifiers to estimate the likelihood of HLA alleles. While  
77 SNP2HLA explicitly uses reference haplotype data, of which public accessibility is often limited,  
78 HIBAG does not require them once the trained models are generated. Both methods have  
79 achieved high imputation accuracy;<sup>16</sup> however, are less accurate for rare alleles as shown later.  
80 Given the complex linkage disequilibrium (LD) structures specific for the MHC region, a more  
81 sophisticated pattern recognition algorithm beyond simple stochastic inference seems to be  
82 necessary to overcome this situation.

83 After boasting of its extremely high accuracy in image recognition, deep learning has  
84 been attracting attention in various fields, and a lot of successful applications in the field of  
85 genomics have been reported.<sup>17</sup> It can learn a representation of input data and discover  
86 relevant features of high complexity through deep neural networks. Its typical application for  
87 genomic problems is the prediction of the effects of non-coding and coding variants, where the  
88 models encodes the inputs of flanking nucleotide sequence data.<sup>18-21</sup> Another example is  
89 non-linear unsupervised learning of high-dimensional quantitative data of transcriptome.<sup>22,23</sup>  
90 However, successful representation learnings for SNV-data in the field of population genetics  
91 has been limited.<sup>24</sup> Here, we developed DEEP\*HLA, a multi-task convolutional deep learning

92 method to accurately impute genotypes of HLA genes from SNV-level data. Through  
93 application to the two HLA reference panels of different populations, DEEP\*HLA achieved  
94 higher imputation accuracy both in sensitivity and specificity than conventional methods.  
95 Notably, it was more advantageous especially in imputing low frequent or rare alleles. As also a  
96 value of our method, it was by far the fastest in total processing time, which indicates its  
97 applicability to biobank-scale data. We applied the trained models of DEEP\*HLA to the  
98 large-scale T1D GWAS data of BioBank Japan (BBJ) and UK Biobank (UKBB), and conducted  
99 trans-ethnic HLA association analysis.

100

101

102 **Results**

103

104 **An overview of our study**

105 An overview of our study is presented in **Fig. 1**. Our method, DEEP\*HLA, is convolutional  
106 neural networks which learn an HLA referenced panel, and impute genotypes of HLA genes  
107 from pre-phased SNV data. Its framework uses a multi-task learning which can learn and  
108 impute alleles of several HLA genes which belong to the same group simultaneously (see  
109 Method). Multi-task learning is presumed to have two advantages in this situation. First, the  
110 genotypes of some flanking HLA genes, which often have strong LD for each other, are  
111 correlated; and the shared features of individual tasks would be informative. Second, it helps  
112 reduce the processing time by grouping tasks especially in our latest reference panel, which  
113 consists of more than thirty HLA genes. For robust benchmarking, we targeted the two different  
114 HLA imputation reference panels: (i) our Japanese reference panel ( $n = 1,118$ );<sup>3</sup> (ii) the Type 1  
115 Diabetes Genetics Consortium (T1DGC) reference panel ( $n = 5,112$ ),<sup>25</sup> respectively. We  
116 evaluated its performance in comparison with other HLA imputation methods by 10-fold  
117 cross-validation and an independent HLA dataset ( $n = 908$ ).<sup>6</sup> In the latter part, we performed  
118 MHC fine-mappings of Japanese cohort from BBJ and British cohort from UKBB by applying  
119 the trained models specific for individual populations. We integrated the imputed GWAS  
120 genotypes and performed trans-ethnic HLA association analysis.

121 **DEEP\*HLA achieved high imputation accuracy especially in low-frequency or rare**  
122 **alleles**

123 First, we applied DEEP\*HLA to the Japanese panel, which is a high-resolution allele catalog  
124 of the 33 classical and non-classical HLA genes in 1,118 individuals of Japanese ancestry.<sup>3</sup> We  
125 compared imputation accuracy of DEEP\*HLA in sensitivity and specificity (see Method) with  
126 SNP2HLA and HIBAG in 10-fold cross-validation. DEEP\*HLA achieved sensitivity and  
127 specificity of 0.987 in 4-digit allelic resolution, which were superior to SNP2HLA (sensitivity of  
128 0.985 and specificity of 0.984) and HIBAG (sensitivity and specificity of 0.979; **Supplementary**  
129 **Table 1**). Remarkably, DEEP\*HLA was best through all ranges of allele frequencies; and was  
130 more advantageous as alleles were low frequent or rare (**Fig. 2a** and **Supplementary Table 1**).  
131 In addition to the cross-validation, to investigate whether DEEP\*HLA could impute well when  
132 applied to independent samples, we applied the model trained with our Japanese reference  
133 panel to a dataset of 908 Japanese individuals (1,816 haplotypes) with 4-digit resolution alleles  
134 of 8 classical HLA genes and SNP genotype data.<sup>6</sup> Similarly, DEEP\*HLA performed better than  
135 the other methods; and was more advantageous as alleles were low frequent or rare (**Fig. 2a**  
136 and **Supplementary Table2**).

137 Next, we applied DEEP\*HLA to the Type 1 Diabetes Genetics Consortium (T1DGC)  
138 reference panel of 5,122 unrelated individuals of European ancestries.<sup>25</sup> It consists of 2- and  
139 4-digit alleles of the 8 classical HLA gene. DEEP\*HLA achieved sensitivity and specificity of  
140 0.976 in 4-digit resolution, which were superior to SNP2HLA (sensitivity of 0.972 and specificity  
141 of 0.935) and HIBAG (sensitivity and specificity of 0.959), was more advantageous as the  
142 alleles were low frequent or rare (**Fig.2b** and **Supplementary Table 3**). There were significant  
143 declines in the specificity of SNP2HLA especially for imputing infrequent alleles, because the

144 sum of the allele dosages of each HLA gene of an individual can exceed the expected value (i.e.  
145 = 2.0) since it imputes each allele separately as a binary allele.

146

#### 147 **DEEP\*HLA can define HLA amino acid polymorphisms without ambiguity**

148 DEEP\*HLA separately imputes classical alleles of each HLA gene, as a multi-label  
149 classification in the field of machine learning. Thus, it has an advantage that the sum of imputed  
150 allele dosages of each HLA gene is definitely set as an ideal value of 1.0 per a haplotype. This  
151 feature enables us to define a dosage of amino acid polymorphisms from the imputed 4-digit  
152 allele dosages without ambiguity. Then, we compared this method of imputing amino acid  
153 polymorphisms with SNP2HLA, which imputes them as binary alleles. Although DEEP\*HLA  
154 was equivalent with SNP2HLA in both accuracy metrics in imputing amino acid polymorphisms  
155 in total (0.997 vs 0.997 in the Japanese panel; 0.996 vs 0.996 in T1DGC panel;  
156 **Supplementary Table 4, 5**), it achieved more accurate imputation for low-frequency and rare  
157 alleles (**Fig. 2c, d**). As well as in imputing classical HLA alleles, the performance improvement  
158 was remarkable in specificity evaluated in T1DGC data.

159

#### 160 **High performance of DEEP\*HLA in computational costs**

161 We benchmarked the computational costs of DEEP\*HLA against SNP2HLA and HIBAG using  
162 subset of GWAS dataset from BBJ containing  $n = 1,000, 2,000, 5,000, 10,000, 20,000, 50,000,$   
163 and 100,000 samples (2,000 SNPs consistent with the reference panel). Unlike SNP2HLA,  
164 DEEP\*HLA and HIBAG require pre-phased GWAS data and the models trained with reference  
165 data. Thus, we compared the total processing time including pre-phasing of GWAS data,  
166 training the models, and imputation of DEEP\*HLA and HIBAG, with the running time of

167 SNP2HLA. We used a state-of-art GPU, GeForce RTX 2080 Ti in training DEEP\*HLA. As  
168 shown in **Fig. 2e**, DEEP\*HLA imputation was by far the fastest in total processing time as the  
169 sample size increased. When comparing the pure imputation times, it was faster than HIBAG  
170 (**Supplementary Table 6**). As for memory cost, all methods exhibited maximum memory usage  
171 scaling roughly linearly with sample size (**Fig. 2e** and **Supplementary Table 6**), and HIBAG  
172 was the most memory-efficient through all the sample sizes. While SNP2HLA did not work  
173 within 100 GB memory of our machine for the sample size of more than 20,000, DEEP\*HLA  
174 was able to impute even the biobank-scale sample size that reached 100,000.

175

### 176 **Characteristics of the alleles where DEEP\*HLA was advantageous to impute**

177 We focused on the characteristics of the HLA alleles of which accuracy was improved by our  
178 method in comparison with SNP2HLA, which was second to our method in total accuracy  
179 metrics. SNP2HLA runs Beagle intrinsically, which performs imputation based on hidden  
180 Markov model of a localized haplotype-cluster. We hypothesized that this kind of methods  
181 works better for imputing alleles of which LDs with the surrounding SNVs are stronger in close  
182 positions and get weaker as more distant from the target HLA allele (we termed this feature as  
183 distant-dependent LD decay). Conversely, it could be limited at imputing alleles which have  
184 sparse LD structures throughout the MHC region. To verify this hypothesis, we defined the area  
185 under curve (AUC) representing distant-dependent LD decay. The AUC values become higher  
186 when LDs with the surrounding SNVs get stronger as they get closer to the target HLA allele  
187 (**Fig. 3b**). We evaluated how much two accuracies of DEEP\*HLA and SNP2HLA are affected  
188 by the AUC values and allele frequency with a multivariate linear regression analysis. As  
189 expected, both sensitivity and specificity were positively correlated with AUC in SNP2HLA. On

190 the other hand, the specificity in DEEP\*HLA were less dependent on AUC, and there was no  
191 significant correlation with the specificity in cross-validation on the Japanese panel ( $P = 0.069$ ;  
192 **Fig. 3a and Supplementary Table 7**).

193 Next, to investigate our assumption that DEEP\*HLA performs better imputation by  
194 recognizing distant SNVs as well as close SNVs of strong LD, we applied SmoothGrad, a  
195 method for generating a sensitivity map of a deep learning model.<sup>26</sup> It is a simple  
196 approach based on the idea of adding noise to the input data and taking the average of the  
197 resulting sensitivity maps for each sampled data. As displayed in its application to example HLA  
198 alleles, a trained DEEP\*HLA model reacted to the noises of not only the surrounding SNVs with  
199 strong LD, but also the distant SNVs (**Fig. 3c**). Interestingly, the strongly reacted SNVs were  
200 not always those of even moderate LD, but also spread across the entire the input region. While  
201 the validity of SmoothGrad for a deep learning model of genomic data has under investigation,  
202 one probable explanation is that predicting an allele by our method conversely means  
203 predicting absence of the other alleles of the target HLA gene; thus, any SNV positions in LD  
204 with any of the other HLA alleles could be informative. Another explanation is that DEEP\*HLA  
205 might recognize complicated combinations of multiple distinct SNVs within the region, rather  
206 than the simple HLA allele-SNV LD correlations.

207

### 208 **Empirical evaluation of imputation uncertainty in deep learning models**

209 A common issue of deep learning models is how to quantify the reliability of their predictions;  
210 and one potential solution is uncertainty inferred from the idea of Bayesian deep learning.<sup>27</sup>  
211 Then, we experimentally evaluated the uncertainty of imputation by DEEP\*HLA using Monte  
212 Carlo (MC) dropout, which could be applied following general implementation of neural

213 networks with dropout units.<sup>28,29</sup> In MC dropout, uncertainty was presented as entropy of  
214 sampling variation with keeping dropout turned on. This uncertainty index corresponds not to  
215 each binary allele of a gene, but to the prediction of genotype of a gene of an individual. Thus,  
216 we evaluated whether it could guess the correctness of best-guess genotypes of the target HLA  
217 genes. We compared it with a dosage-based discrimination, in which we assume that a  
218 best-guess imputation of higher genotype dosage (probability) is more likely to be correct. The  
219 entropy-based uncertainty identified incorrectly imputed genotypes in areas under the curve of  
220 the receiver operating characteristic (ROC-AUC) of 0.851 in the Japanese panel, and of 0.883  
221 in T1DGC reference panel in 4-digit alleles, which were superior to dosage-based  
222 discrimination (ROC-AUC = 0.722 in the Japanese panel and = 0.754 in T1DGC panel;  
223 **Supplementary Fig. 1**). Whereas the estimation of prediction uncertainty of a deep learning  
224 model is still developing;<sup>29</sup> our results might illustrate its potential applicability to establishment  
225 of a reliability score for genotype imputation by deep neural networks.

226

### 227 **Trans-ethnic MHC fine-mapping of T1D**

228 We applied the DEEP\*HLA models trained with the Japanese panel and T1DGC panel to HLA  
229 imputation of T1D GWAS data of BBJ (831 cases and 61,556 controls) and UKBB (732 cases  
230 and 356,123 controls), respectively. T1D is a highly heritable autoimmune disease that results  
231 from T cell-mediated destruction of insulin-producing pancreatic  $\beta$  cells.<sup>30</sup> We separately  
232 imputed GWAS data of the cohorts and then combined them to perform trans-ethnic MHC  
233 fine-mapping (1,563 cases and 417,679 controls). Association analysis of the imputed HLA  
234 variants with T1D found the most significant association at the HLA-DR $\beta$ 1 amino acid position  
235 71 ( $P_{\text{omnibus}} = P = 6.2 \times 10^{-119}$ ; **Fig. 4a and Supplementary Table 8**), one of the T1D risk amino

236 acid polymorphisms in the European population.<sup>10</sup> In T1D, the largest HLA gene associations  
237 were reported in the *HLA-DRB1*, *-DQA1*, and *-DQB1*;<sup>10,31</sup> thus, we further investigated  
238 independently associated variants within these HLA genes. When conditioning on HLA-DRβ1  
239 amino acid position 71, we observed the most significant independent association in HLA-DQβ1  
240 amino acid position 185 ( $P_{\text{omnibus}} = 8.9 \times 10^{-69}$ ). Through stepwise forward conditional analysis  
241 in the class II HLA region, we found significant independent associations in on Tyr30 in  
242 HLA-DQβ1 ( $P_{\text{binary}} = 9.6 \times 10^{-20}$ ), HLA-DRβ1 amino acid position 74 ( $P_{\text{omnibus}} = 1.4 \times 10^{-11}$ ), and  
243 Arg70 in HLA-DQβ1 ( $P_{\text{omnibus}} = 4.5 \times 10^{-9}$ ; **Supplementary Fig.2** and **Supplementary Table 9**).  
244 The association of HLA-DRβ1 amino acid position 74 has been previously reported in  
245 Europeans.<sup>32</sup>

246 These results were different from a previous study of large T1D cohort of European  
247 ancestries, which reported three amino acid polymorphisms at HLA-DQβ1 position 57,  
248 HLA-DRβ1 position 13, and HLA-DRβ1 position 71 were top-associated amino acid  
249 polymorphisms in the *HLA-DRB1*, *-DQA1*, and *-DQB1* region. We then constructed multivariate  
250 regression models for individual population that incorporated our T1D risk-associated HLA  
251 amino acid polymorphisms and classical alleles of *HLA-DRB1* and *HLA-DQB1*, and compared  
252 the effects of these variants. Whereas the odds ratios of the risk-associated variants reported  
253 previously did not show any positive correlation between different populations (Pearson's  $r =$   
254  $-0.59$ ,  $P = 0.058$ ; **Supplementary Fig.3** and **Supplementary Table 10**), those observed in our  
255 analyses presented significant positive correlation (Pearson's  $r = 0.76$ ,  $P = 6.8 \times 10^{-3}$ ;  
256 **Supplementary Fig.3**).

257 We further investigated whether T1D risk was associated with other HLA genes  
258 independently of *HLA-DRB1*, *-DQA1*, and *-DQB1*. When conditioning on *HLA-DRB1*, *-DQA1*,

259 and *-DQB1*, we identified a significant independent association at HLA-A amino acid position 62  
260 ( $P_{\text{omnibus}} = 5.4 \times 10^{-13}$ ; **Fig. 4b** and **Supplementary Table 8**). After conditioning on HLA-A  
261 amino acid position 62, we did not observe any additional independent association in HLA-A  
262 alleles. When we conditioned on *HLA-DRB1*, *-DQA1*, *-DQB1*, and *-A*, we identified a significant  
263 independent association at HLA-B\*54:01 ( $P_{\text{binary}} = 1.3 \times 10^{-9}$ ; **Fig. 4c** and **Supplementary**  
264 **Table 8**), and its unique amino acid alleles (Gly45 and Val52 at HLA-B). HLA-B\*54:01 has  
265 traditionally been suggested as a risk allele in Japanese by a candidate HLA gene approach.<sup>11</sup>  
266 Its independent association through the MHC region-wide fine-mapping was first proven  
267 here. When conditioning on *HLA-DRB1*, *-DQA1*, *-DQB1*, *-A*, and *-B*, no variants in the MHC  
268 region satisfied the genome-wide significance threshold ( $P > 5.0 \times 10^{-8}$ ; **Fig. 4d** and  
269 **Supplementary Table 8**). Multivariate regression analysis of the identified risk variants  
270 explained 10.3% and 27.6% of the phenotypic variance in T1D under assumption of disease  
271 prevalence of 0.014%<sup>33</sup> and 0.4%<sup>34</sup> for Japanese and British cohorts, respectively. Their odds  
272 ratios on T1D risk were also correlated between different populations (Pearson's  $r = 0.71$ ,  $P =$   
273  $4.4 \times 10^{-3}$ ; **Table 1**).

274 **Discussion**

275 In this study, we demonstrated that DEEP\*HLA, a multi-task convolutional deep learning  
276 method for HLA imputation, outperformed conventional HLA imputation methods both in  
277 sensitivity and specificity. DEEP\*HLA was more advantageous when the target HLA variants,  
278 including classical alleles and amino acid polymorphisms, were low frequent or rare. Our study  
279 demonstrated that a conventional method dropped its performance for the alleles which did not  
280 exhibit distant-dependent LD decay features with the target HLA allele. DEEP\*HLA was not  
281 restricted to this point, and comprehensively captures the relationships among distinct multiple  
282 variants regardless of LD.

283 To date, technical application of deep neural networks to population genetics data has  
284 been limited. In a previous attempt for genotype imputation, a sparse convolutional denoising  
285 autoencoder was only compared with reference-free methods.<sup>24</sup> There might be two possible  
286 reasons for the success of our DEEP\*HLA. First unlike genotype imputation by denoising  
287 autoencoders, which assumed various positions of missing genotypes in a reference panel to  
288 impute, the prediction targets were fixed to the HLA allele genotypes as a classification problem.  
289 Second, convolutional neural networks, which leverage a convolutional kernel that is capable of  
290 learning various local patterns, might be suited for learning the complicated LD structures of the  
291 MHC region.

292 We filtered alleles of poor imputation quality based on the results of cross-validation in  
293 the current application; however, an indicator of reliability could be further utilized. We  
294 demonstrated that the uncertainty of prediction inferred from a Bayesian deep learning method  
295 had potential capability of distinguishing incorrectly-imputed alleles in per-gene of individuals.

296 Our future work should establish a method to quantify per-allele uncertainty of imputation which  
297 could be practically used as a filtering threshold for subsequent analyses.

298 Taking advantage of the significant improvement of imputation accuracy for rare  
299 alleles, we conducted trans-ethnic MHC fine-mapping in T1D. Our study successfully  
300 disentangled a set of independently associated amino acid polymorphisms and HLA alleles.  
301 This approach could be performed as well using the conventional HLA imputation methods.  
302 However, the results obtained by our method should be more reliable since there were several  
303 risk-associated alleles which were rare only in one population. As a result, the catalogue of the  
304 T1D risk-associated variants by our trans-ethnic approach were different from those of the  
305 previous study in Europeans.<sup>10</sup> We admit the possibility that the smaller sample size in our  
306 study and different definition of the phenotypes (between studies, and between cohorts in our  
307 study) might also contribute to this disparity. Especially, we note potential distinctiveness of  
308 Japanese T1D phenotypes.<sup>35</sup> Considering that our observed variants shared the effects on the  
309 T1D risk between different populations, however, we might gain a novel insight into the issue of  
310 inter-ethnic heterogeneity of T1D risk allele in the MHC region.

311 In terms of trans-ethnic analysis, we targeted the two major populations of Europeans  
312 and east Asians. As a next step, multi-ethnic MHC fine-mapping integrating further diverse  
313 ancestry should be warranted for robust prioritization of risk-associated HLA variants.<sup>13</sup> Given  
314 their high learning capacity of deep neural networks, our method should be helpful not only  
315 when integrating the imputation results of multiple references, but also when using a more  
316 comprehensive multi-ethnic reference. We expect that highly accurate imputation realized by  
317 learning of complex LDs in the MHC region using neural networks will enable us to further

318 elucidate the involvement of common genetic features in the MHC region that affect complex  
319 traits beyond ethnicity.

320

### 321 **Acknowledgements**

322 We would like to thank all the participants involvement in this study. We thank the members of  
323 Biobank Japan and RIKEN Center for Integrative Medical Sciences for their supports on this  
324 study.

325

### 326 **Conflicts of interests**

327 The authors declare no conflicts of interests.

328

### 329 **Data availability**

330 The Japanese HLA data have been deposited at the National Bioscience Database Center  
331 (NBDC) Human Database (research ID: hum0114). Independent HLA genotype data of  
332 Japanese population is available in the Japanese Genotype-phenotype archive (JGA;  
333 accession ID: JGAS00000000018). T1DGC HLA reference panel can be download at a NIDDK  
334 central repository with a request (<https://repository.niddk.nih.gov/studies/t1dgc-special/>).  
335 GWAS data of the BBJ are available at the NBDC Human Database (research ID: hum0014).  
336 UKBB GWAS data is available upon request (<https://www.ukbiobank.ac.uk/>).

337

### 338 **Code availability**

339 Python scripts for training a model and performing imputation with our method are in  
340 DEEP\*HLA GitHub repository (<https://github.com/tatsuhikonaito/DEEP-HLA>).

341 **Methods**

342 **The architecture of DEEP\*HLA**

343 DEEP\*HLA is a multitask convolutional neural network with a shared part of two convolutional  
344 layers and a fully-connected layer, and individual fully-connected layers which output allelic  
345 dosages of individual HLA genes to impute simultaneously HLA genes of the same group  
346 (**Supplementary Fig.4**). The grouping was based on the LD structure<sup>3</sup> and physical distance in  
347 the current application: (1) {*HLA-F*, *HLA-V*, *HLA-G*, *HLA-H*, *HLA-K*, *HLA-A*, *HLA-J*, *HLA-L*,  
348 *HLA-E*}, (2) {*HLA-C*, *HLA-B*, *MICA*, *MICB*}, (3) {*HLA-DRA*, *HLA-DRB9*, *HLA-DRB5*, *HLA-DRB4*,  
349 *HLA-DRB3*, *HLA-DRB8*, *HLA-DRB7*, *HLA-DRB6*, *HLA-DRB2*, *HLA-DRB1*, *HLA-DQA1*,  
350 *HLA-DOB*, *HLA-DQB1*}, and (4) {*TAP2*, *TAP1*, *HLA-DMB*, *HLA-DMA*, *HLA-DOA*, *HLA-DPA1*,  
351 *HLA-DPB1*}. Genes which were not typed or had only one allele in individual reference panels  
352 were excluded from the group.

353 For each group, SNPs within its window are encoded to one-hot vectors based on  
354 whether each genotype is consistent with a reference or alternative allele. The window sizes on  
355 each side were set to 500 kb in the current investigation. Two convolutional layers with  
356 max-pooling layers and a fully-connected layer follow the input layer as a shared part. The  
357 fully-connected layer in the end of shared part is followed by each fully-connected layer which  
358 has nodes consistent with the number of alleles of each HLA gene. To return a dosage of  
359 imputation, which ranges from 0.0 to 1.0 for a haplotype, softmax activation was added before  
360 the last output. Dropout was used on the convolutional and fully-connected layers,<sup>36</sup> and batch  
361 normalization was added to the convolutional layers.<sup>37</sup>

362 During training, 5% of data set were spared for validation to determine the point for  
363 early-stopping training (i.e. we used 85% of data were used for training in 10-fold

364 cross-validation). Categorical cross entropy loss function of each HLA gene was minimized  
365 using the Adam optimizing algorithm.<sup>38</sup> As a multi-task learning to find a Pareto optimal solution  
366 of all tasks, we used the multiple-gradient descent algorithm – upper bound (MGDA-UB), where  
367 the loss function of each task is scaled based on its optimization algorithms.<sup>39</sup> To taking  
368 advantage of the hierarchical nature of HLA alleles (i.e. 2-digit, 4-digit, and 6-digit), we  
369 implemented hierarchical fine-tuning, in which the parameters of model of upper hierarchical  
370 structures were transferred to those of the lower one.<sup>40</sup> We transferred the parameters of  
371 shared networks of 2-digit alleles to 4-digit alleles, and of 4-digit alleles to 6-digit alleles during  
372 training successively. Although some HLA alleles in our reference panel were not determined in  
373 4-digit or 6-digit resolution, we set their upper resolution instead to keep equivalent hierarchical  
374 levels with other HLA genes. Hyperparameters, including the number of filters and kernel sizes  
375 of convolutional layers, fully-connected layer size, were tuned with Optuna.<sup>41</sup> The  
376 hyperparameters of the Japanese model were determined using an randomly sampled set  
377 before cross-validation, and the same values were used for hyper-parameters of the European  
378 model. Our deep learning architectures were implemented using Pytorch 1.4.1 (see URLs), a  
379 Python neural network library.

380

### 381 **Empirical evaluation of HLA imputation accuracy**

382 We defined two metrics to evaluate the imputation accuracy of the gene-level dosage in various  
383 aspects. First, the accuracy was calculated by summing across all individuals the dosage of  
384 each true allele in the individual, and divided by the total number of observation, as proposed in  
385 the paper of SNP2HLA.<sup>25</sup> We defined this as sensitivity  $Se$  because it counts positives that are  
386 correctly identified as such.

$$Se(L) = \frac{\sum_{i=1}^n (D_i(A1_{i,L}) + D_i(A2_{i,L}))}{2n}$$

387 where  $n$  denotes the number of individuals,  $D_i$  represents the imputed dosage of an allele in  
388 individual  $i$ , and alleles  $A1_{i,L}$  and  $A2_{i,L}$  represent the true HLA alleles for individual  $i$  at locus  $L$ .

389 In contrast, we defined specificity  $Sp$  as

$$Sp(L) = 1 - \frac{\sum_{i=1}^n (D_i(\overline{A1_{i,L}}) + D_i(\overline{A2_{i,L}}))}{2n}$$

390 where alleles  $\overline{A1_{i,L}}$  and  $\overline{A2_{i,L}}$  represent the HLA alleles which are incorrectly imputed dosage  
391 for individual  $i$  at locus  $L$ . Due to the nature of formula, total sensitivity and specificity of each  
392 HLA gene should be the same value for DEEP\*HLA and HIBAG, in which the sum of dosage in  
393 each HLA gene of each individual is constant.

394 We extended these metrics for each gene to evaluate imputation performance of each  
395 allele  $A$ .

$$Se(A) = \frac{\sum_{j=1}^m D_j(A)}{m}$$

$$Sp(A) = 1 - \frac{\sum_{k=1}^{2n-m} D_k(A)}{m}$$

396 where  $m$  denotes the number of true observations of allele  $A$  in total sample, and  $D_j$  represents  
397 imputed dosage of allele  $A$  in individual haplotype  $j$  which has allele  $A$ .  $D_k$  represents imputed  
398 dosage of allele  $A$  in individual haplotype  $k$  of which true allele is not  $A$  (note,  $Sp(A)$  can be a  
399 negative value). Although these metrics are different from their general definitions, they are  
400 adjusted for bias due to allele frequency by dividing by true number of alleles.

401 When averaging the accuracy metrics, we weighted them by allele frequency.

402

403 **Estimation of HLA imputation uncertainty of DEEP\*HLA using MC dropout method**

404 In order to provide uncertainty of prediction, we adopted the entropy of sampling variation of MC  
405 dropout method.<sup>28</sup> In MC dropout, dropout are kept during prediction to perform multiple model  
406 calls. Different units are dropped across different model calls; thus, it can be considered as  
407 Bayesian sampling with treating the parameters of a CNN model as random variables of  
408 Bernoulli distribution. The uncertainty of a best-guess genotype inferred from the entropy of  
409 sampling variation is determined as

$$H = -\left(\frac{t}{T} \log \frac{t}{T} + \frac{T-t}{T} \log \frac{T-t}{T}\right)$$

410 where  $T$  is the number of variational samplings and  $t$  is the number of times in which obtained  
411 genotype was same as the best-guess genotype. We set  $T = 200$  in the current investigation.

412

### 413 **AUC metric representing distant-dependent LD decay**

414 To evaluate whether the LD between an HLA allele and its surrounding SNVs gets weaker as  
415 the SNVs are distant to it, we calculated the area under the curve (AUC) of the cumulative curve  
416 of  $r^2$  from the HLA allele (AUC for distance-dependent LD decay). When the LD of flanking  
417 SNVs of an HLA allele has such a characteristic,  $r^2$  measure of LD tends to decline from the  
418 HLA allele. In other words, the bilateral cumulative curve of  $r^2$  from the HLA allele should be  
419 more likely to be convex upward; then the AUC tends to be higher. We determined the AUC by  
420 normalizing the maximum values of  $r^2$  sum and window sizes to 1. We evaluated its association  
421 with accuracies of each imputation method by linear regression model adjusted with an allele  
422 frequency and the maximum value of  $r^2$ . We set window size as the range of its input for  
423 evaluating the association with DEEP\*HLA, and 1,000 for SNP2HLA.

424

### 425 **Regional sensitivity maps of DEEP\*HLA**

426 We applied SmoothGrad approach to estimate which SNVs were important for DEEP\*HLA to  
427 impute genotypes of each HLA gene.<sup>26</sup> For each haplotype, we generated 200 samples which  
428 were added Gaussian noise to encoded SNV data and input them to a trained model, and  
429 obtained the sensitivity values for individual SNV positions by averaging the absolute values of  
430 gradients caused by the difference from the true label. When we obtained the sensitivity of an  
431 allele, we averaged the maps of all haplotypes which truly has the allele.

432

### 433 **HLA imputation software and parameter settings**

434 We tested the latest version of each software available in Jun 2020 to compare with our method.  
435 SNP2HLA (v1.0.3) first arranges the strand in its own algorithm; however, we removed this step  
436 data during cross-validation, in which the strands must be the same between training and test  
437 data. Other settings of SNP2HLA were set to the default values. HIBAG (1.22.0.) receives  
438 phased genotypes data as input; and we used phased data generated using Beagle as well as  
439 our method. The number of classifiers were set to 25, which is sufficient to provide good  
440 performance,<sup>42</sup> in testing with the Japanese. For T1DGC panel, training time was extremely  
441 long with 25 classifiers; thus, we set 2 of classifiers after we confirmed that the imputation  
442 accuracy was almost unchanged in the first set of cross-validation. Flanking regions on each  
443 side was set to 500 kb.

444

### 445 **Computational costs measurement**

446 We measured the computational costs of imputation of subset of BioBank Japan (BBJ) Project  
447 data set ( $n = 1,000, 2,000, 5,000, 10,000, 20,000, 50,000,$  and  $100,000$  samples) by our  
448 Japanese reference panel (2,000 SNVs were consistent). All our runtime analyses except

449 model training of DEEP\*HLA were performed on a dedicated server running CentOS 7.2.1511,  
450 with 48 CPU cores (Intel® Xeon® E5-2687W v4 @ 3.00 GHz) and 256 GB of RAM without  
451 GPU. The model training of DEEP\*HLA was conducted on Ubuntu 16.04.6 LTS with 20 CPU  
452 cores (Intel® Core™ i9-9900X @ 3.50 GHz), 2 GPUs (NVIDIA® GeForce® RTX 2080 Ti),  
453 and 128 GB of RAM. DEEP\*HLA and HIBAG require pre-phased GWAS data and the models  
454 trained with reference data; thus, we measured the process not only of imputation, but also of  
455 pre-phasing of GWAS data (conducted by Eagle) and training the models with a reference  
456 panel. In SNP2HLA, the maximum of available memory was set to 100 GB. The processing  
457 time and maximum memory usage was measured using GNU Time software when running  
458 from a command line interface.

459

#### 460 **HLA imputation reference data**

461 (i) Our Japanese reference panel and a validation dataset

462 Our Japanese reference panel contains NGS-based 6-digit resolution HLA typing data of 33  
463 classical and non-classical HLA genes, of which 9 were classical HLA genes (*HLA-A*, *HLA-B*,  
464 and *HLA-C* for class I; *HLA-DRA*, *HLA-DRB1*, *HLA-DQA1*, *HLA-DQB1*, *HLA-DPA1*, and  
465 *HLA-DPB1* for class II) and 24 were nonclassical HLA genes (*HLA-E*, *HLA-F*, *HLA-G*, *HLA-H*,  
466 *HLA-J*, *HLA-K*, *HLA-L*, *HLA-V*, *HLA-DRB2*, *HLA-DRB3*, *HLA-DRB4*, *HLA-DRB5*, *HLA-DRB6*,  
467 *HLA-DRB7*, *HLA-DRB8*, *HLA-DRB9*, *HLA-DOA*, *HLA-DOB*, *HLA-DMA*, *HLA-DMB*, *MICA*, *MICB*,  
468 *TAP1*, and *TAP2*), along with high-density SNP data of the MHC region by genotyping with the  
469 Illumina HumanCoreExome BeadChip (v1.1; Illumina) of 1,120 unrelated individuals of  
470 Japanese ancestry.<sup>3</sup> Among them, we excluded 2 individuals' data in which sides of some HLA  
471 alleles were inconsistent among different resolutions after pre-phasing.

472 To benchmark the imputation performance when the Japanese panel is applied to  
473 independent dataset, we used 908 individuals of Japanese ancestries with 4-digit resolution  
474 alleles of classical HLA genes (*HLA-A*, *HLA-B*, *HLA-C*, *HLA-DRB1*, *HLA-DQA1*, *HLA-DQB1*,  
475 *HLA-DPA1*), which was used as a HLA reference panel in our previous study.<sup>6</sup> It contains  
476 high-density SNP data genotyped with four SNP genotyping arrays (the Illumina  
477 HumanOmniExpress BeadChip, the Illumina HumanExome BeadChip, the Illumina  
478 ImmunoChip, and the Illumina HumanHap550v3 Genotyping BeadChip). This study was  
479 approved by the ethical committee of Osaka University Graduate School of Medicine.

480 (ii) The Type 1 Diabetes Genetics Consortium (T1DGC) reference panel.

481 T1DGC panel contains 5,868 SNPs (genotyped with Illumina ImmunoChip) and 4-digit  
482 resolution HLA typing data of classical HLA genes (*HLA-A*, *HLA-B*, and *HLA-C* for class I,  
483 *HLA-DPA1*, *HLA-DPB1*, *HLA-DQA1*, *HLA-DQB1*, and *HLA-DRB1* for class II) of 5,225  
484 unrelated individuals of European ancestries.<sup>14</sup> Among them, we excluded 103 individuals' data  
485 in which sides of some HLA alleles were inconsistent among different resolutions after  
486 pre-phasing.

487

### 488 **T1D GWAS data in the Japanese population**

489 The BioBank Japan (BBJ) is a multi-institutional hospital-based registry that comprised DNA,  
490 serum, and clinical information of approximately 200,000 individuals of Japanese ancestry in  
491 2003-2007.<sup>43,44</sup> We used GWAS data from 831 cases who had record of T1D diagnosis and  
492 61,556 controls of Japanese genetic ancestry enrolled in BBJ Project. The controls were  
493 included in those enrolled in our previous study that investigated the association of the MHC  
494 region to comprehensive phenotypes, and the number of T1D cases was increased.<sup>3</sup> The

495 process of patient registration, the GWAS data, and the QC process have been described  
496 elsewhere.<sup>43–45</sup>

497

### 498 **T1D GWAS data in the British population**

499 The UK Biobank (UKBB) comprises health related information approximately 500,000  
500 individuals aged between 40-69 who were recruited from across the United Kingdom in  
501 2006-2010.<sup>46</sup> We used GWAS data from 732 T1D patients and 356,123 controls of British  
502 genetic ancestry enrolled in UKBB. We selected T1D patients as individuals who were  
503 diagnosed as insulin-dependent diabetes mellitus in hospital records, and neither as  
504 non-insulin-independent diabetes mellitus in hospital records nor as type 2 diabetes in  
505 self-reported diagnosis. The controls were selected as individuals who did not have record of  
506 any autoimmune diseases neither in hospital records nor in self-reported diagnosis. We  
507 included only individuals of British ancestry according to self-identification and criteria based on  
508 principal component (PC).<sup>47</sup> We excluded individuals of ambiguous sex (sex chromosome  
509 aneuploidy and inconsistency between self-reported and genetic sex), and outlier of  
510 heterozygosity or call rate of high quality markers.

511

### 512 **Imputation of the HLA variants of GWAS data of T1D and control individuals**

513 In this study, we defined the HLA variants as SNVs in the MHC region, classical 2-digit and  
514 4-digit biallelic HLA alleles, biallelic HLA amino acid polymorphisms corresponding to the  
515 respective residues, and multi-allelic HLA amino acid polymorphisms for each amino acid  
516 position. We applied DEEP\*HLA to the GWAS data to determine classical 2-digit and 4-digit  
517 biallelic HLA alleles. The dosages of biallelic HLA amino acid polymorphisms corresponding to

518 the respective residues and multiallelic HLA amino acid polymorphisms for each amino acid  
519 position were determined from the imputed 4-digit classical allele dosages. We applied  
520 post-imputation filtering as the biallelic alleles of which both the sensitivity and specificity in  
521 10-fold cross-validation were higher than 0.7. The sensitivity and specificity of the current  
522 definition could be overestimated if an allele frequency is above 0.5; thus, we calculated those  
523 with allele reversed (i.e. flipping reference/alternative alleles) and filtered also by them. The  
524 SNVs in the MHC region were imputed using minimac3 (version 2.0.1) after pre-phased with  
525 Eagle (version 2.3). We applied stringent post-imputation QC filtering of the variants (minor  
526 allele frequency  $\geq 0.5\%$  and imputation score  $R_{sq} \geq 0.7$ ). For trans-ethnic fine-mapping, we  
527 integrated the results of imputation of individual cohorts by including the HLA genes, amino acid  
528 position, and SNVs which were typed in both reference panels. Regarding the HLA alleles and  
529 amino acid polymorphisms that existed in one population, they were regarded as absent on the  
530 other population. Considering the disparity in allele frequency of SNVs among different  
531 populations, we removed all palindromic SNVs to align the strands correctly without fail.

532

### 533 **Association testing of the HLA variants**

534 We assumed additive effects of the allele dosages on the log-odds scale for susceptibility of  
535 T1D; and evaluated associations of the HLA variants with the risk of T1D using a logistic  
536 regression model. To robustly account for potential population stratification, we included the top  
537 ten PCs obtained from the GWAS genotype data of each cohort (not including the MHC region)  
538 as covariates in the regression model. For trans-ethnic analysis, PC terms of each other  
539 population were set to 0; and, besides, we added a categorical variable indicating a population  
540 as a covariate. We also included sex of individuals as a covariate.

541 To evaluate independent risk among the HLA variants and genes, we conducted a  
542 forward-type stepwise conditional regression analysis that additionally included the binary HLA  
543 variant genotypes as covariates. When conditioned on HLA gene(s), we included all the 4-digit  
544 alleles as covariates to robustly condition the associations attributable to the HLA genes, as  
545 previously described.<sup>3,12</sup> When conditioning on the specific HLA amino acid position(s), we  
546 included the multi-allelic variants of the amino acid residues. We applied a forward stepwise  
547 conditional analysis for the HLA variants and then HLA genes, based on the genome-wide  
548 association significance threshold ( $P = 5.0 \times 10^{-8}$ ).

549 We tested a multivariate full regression model by including the risk-associated HLA  
550 variants in *HLA-DRB1*, *HLA-DQB1*, *HLA-A*, and *HLA-B*, which were identified through the  
551 stepwise regression analysis. When we included amino acid polymorphisms in the model, we  
552 excluded the most frequent residue in the British cohort from each amino acid position as the  
553 reference allele. The phenotypic variance explained by the identified risk-associated HLA  
554 variants was estimated on the basis of a liability threshold model assuming the  
555 population-specific prevalence of T1D and using the effect sizes obtained from the multivariate  
556 regression model.

557

## 558 **URLs**

559 DEEP\*HLA, <https://github.com/tatsuhikonaito/DEEP-HLA>

560 Pytorch, <http://pytorch.org/>

561 SNP2HLA, <http://software.broadinstitute.org/mpg/snp2hla/>

562 HIBAG, <https://www.bioconductor.org/packages/release/bioc/html/HIBAG.html>

563 Eagle, <https://data.broadinstitute.org/alkesgroup/Eagle/>

- 564 Minimac3, <https://genome.sph.umich.edu/wiki/Minimac3>
- 565 Biobank Japan, <https://biobankjp.org/english/index.html>
- 566 UK biobank, <https://www.ukbiobank.ac.uk/>

567 **References**

- 568 1. Dendrou, C. A., Petersen, J., Rossjohn, J. & Fugger, L. HLA variation and disease. *Nat.*  
569 *Rev. Immunol.* **18**, 325–339 (2018).
- 570 2. Erlich, H. HLA DNA typing: Past, present, and future. *Tissue Antigens* **80**, 1–11 (2012).
- 571 3. Hirata, J. *et al.* Genetic and phenotypic landscape of the major histocompatibility complex  
572 region in the Japanese population. *Nat. Genet.* **51**, 470–480 (2019).
- 573 4. International HIV Controllers Study *et al.* The major genetic determinants of HIV-1 control  
574 affect HLA class I peptide presentation. *Science* **330**, 1551–1557 (2010).
- 575 5. Raychaudhuri, S. *et al.* Five amino acids in three HLA proteins explain most of the  
576 association between MHC and seropositive rheumatoid arthritis. *Nat. Genet.* **44**, 291–296  
577 (2012).
- 578 6. Okada, Y. *et al.* Construction of a population-specific HLA imputation reference panel and  
579 its application to Graves' disease risk in Japanese. *Nat. Genet.* **47**, 798–802 (2015).
- 580 7. Gourraud, P. A. *et al.* HLA diversity in the 1000 genomes dataset. *PLoS One* **9**, (2014).
- 581 8. Okada, Y. *et al.* Risk for ACPA-positive rheumatoid arthritis is driven by shared HLA  
582 amino acid polymorphisms in Asian and European populations. *Hum. Mol. Genet.* **23**,  
583 6916–6926 (2014).
- 584 9. Todd JA, Bell JI & McDevitt HO. HLA-DQBeta gene contributes to susceptibility and  
585 resistance to insulin-dependent diabetes mellitus. *Nature* **329**, 599–604 (1987).
- 586 10. Hu, X. *et al.* Additive and interaction effects at three amino acid positions in HLA-DQ and  
587 HLA-DR molecules drive type 1 diabetes risk. *Nat. Genet.* **47**, 898–905 (2015).
- 588 11. Kawabata, Y. *et al.* Differential association of HLA with three subtypes of type 1 diabetes:  
589 Fulminant, slowly progressive and acute-onset. *Diabetologia* **52**, 2513–2521 (2009).

- 590 12. Okada, Y. *et al.* Contribution of a Non-classical HLA Gene, HLA-DOA, to the Risk of  
591 Rheumatoid Arthritis. *Am. J. Hum. Genet.* **99**, 366–374 (2016).
- 592 13. Luo, Y. *et al.* A high-resolution HLA reference panel capturing global population diversity  
593 enables multi-ethnic fine-mapping in HIV host response. Preprint at  
594 <https://www.medrxiv.org/content/10.1101/2020.07.16.20155606v1> (2020).
- 595 14. Jia, X. *et al.* Imputing Amino Acid Polymorphisms in Human Leukocyte Antigens. *PLoS*  
596 *One* **8**, (2013).
- 597 15. Levin, A. M. *et al.* Performance of HLA allele prediction methods in African Americans for  
598 class II genes HLA-DRB1, -DQB1, and -DPB1. *BMC Genet.* **15**, 1–11 (2014).
- 599 16. Karnes, J. H. *et al.* Comparison of HLA allelic imputation programs. *PLoS One* **12**, 1–12  
600 (2017).
- 601 17. Eraslan, G., Avsec, Ž., Gagneur, J. & Theis, F. J. Deep learning: new computational  
602 modelling techniques for genomics. *Nat. Rev. Genet.* **20**, 389–403 (2019).
- 603 18. Alipanahi, B., DeLong, A., Weirauch, M. T. & Frey, B. J. Predicting the sequence  
604 specificities of DNA- and RNA-binding proteins by deep learning. *Nat Biotechnol* **33**,  
605 831–838 (2015).
- 606 19. Zhou, J. *et al.* Deep learning sequence-based ab initio prediction of variant effects on  
607 expression and disease risk. *Nat. Genet.* **50**, 1171–1179 (2018).
- 608 20. Sundaram, L. *et al.* Predicting the clinical impact of human mutation with deep neural  
609 networks. *Nat. Genet.* **50**, 1161–1170 (2018).
- 610 21. Naito, T. Predicting the impact of single nucleotide variants on splicing via  
611 sequence-based deep neural networks and genomic features. *Hum. Mutat.* **40**,  
612 1261-1269 (2019).

- 613 22. Riesselman, A. J., Ingraham, J. B. & Marks, D. S. Deep generative models of genetic  
614 variation capture the effects of mutations. *Nat. Methods* **15**, 816–822 (2018).
- 615 23. Dwivedi, S. K., Tjörnberg, A., Tegnér, J. & Gustafsson, M. Deriving disease modules from  
616 the compressed transcriptional space embedded in a deep autoencoder. *Nat. Commun.*  
617 **11**, (2020).
- 618 24. Chen, J. & Shi, X. Sparse convolutional denoising autoencoders for genotype imputation.  
619 *Genes (Basel)*. **10**, 1–16 (2019).
- 620 25. Han, B. *et al.* Fine mapping seronegative and seropositive rheumatoid arthritis to shared  
621 and distinct HLA alleles by adjusting for the effects of heterogeneity. *Am. J. Hum. Genet.*  
622 **94**, 522–532 (2014).
- 623 26. Smilkov, D., Thorat, N., Kim, B., Viégas, F. & Wattenberg, M. SmoothGrad: removing  
624 noise by adding noise. Preprint at <https://arxiv.org/abs/1706.03825> (2017).
- 625 27. Kendall, A. & Gal, Y. What uncertainties do we need in Bayesian deep learning for  
626 computer vision? *Adv. Neural Inf. Process. Syst.* **2017-Decem**, 5575–5585 (2017).
- 627 28. Gal, Y. & Ghahramani, Z. Bayesian Convolutional Neural Networks with Bernoulli  
628 Approximate Variational Inference. Preprint at <https://arxiv.org/abs/1506.02158> (2015).
- 629 29. Gal, Y. & Ghahramani, Z. Dropout as a Bayesian approximation: Representing model  
630 uncertainty in deep learning. *33rd Int. Conf. Mach. Learn. ICML 2016* **3**, 1651–1660  
631 (2016).
- 632 30. Atkinson, M. A., Eisenbarth, G. S. & Michels, A. W. Type 1 diabetes. *Lancet* **383**, 69–82  
633 (2014).
- 634 31. Erlich, H. *et al.* HLA DR-DQ haplotypes and genotypes and type 1 diabetes risk analysis  
635 of the type 1 diabetes genetics consortium families. *Diabetes* **57**, 1084–1092 (2008).

- 636 32. Cucca, F. A correlation between the relative predisposition of MHC class II alleles to type  
637 1 diabetes and the structure of their proteins. *Hum. Mol. Genet.* **10**, 2025–2037 (2001).
- 638 33. Onda, Y. *et al.* Incidence and prevalence of childhood-onset Type 1 diabetes in Japan:  
639 the T1D study. *Diabet. Med.* **34**, 909–915 (2017).
- 640 34. Sivertsen, B., Petrie, K. J., Wilhelmsen-Langeland, A. & Hysing, M. Mental health in  
641 adolescents with Type 1 diabetes: Results from a large population-based study. *BMC*  
642 *Endocr. Disord.* **14**, 1–8 (2014).
- 643 35. Kawasaki, E. & Eguchi, K. Is type 1 diabetes in the Japanese population the same as  
644 among Caucasians? *Ann. N. Y. Acad. Sci.* **1037**, 96–103 (2004).
- 645 36. Srivastava, N., Hinton, G. E., Krizhevsky, A., Sutskever, I. & Salakhutdinov, R. Dropout□:  
646 A Simple Way to Prevent Neural Networks from Overfitting. *J. Mach. Learn. Res.* **15**,  
647 1929–1958 (2014).
- 648 37. Ioffe, S. & Szegedy, C. Batch normalization: Accelerating deep network training by  
649 reducing internal covariate shift. *Proc. ICML* 448–456 (2015).
- 650 38. Kingma, D. & Ba, J. Adam: A method for stochastic optimization. *Int. Conf. Learn.*  
651 *Represent.* (2015).
- 652 39. Sener, O. & Koltun, V. Multi-task learning as multi-objective optimization. *Adv. Neural Inf.*  
653 *Process. Syst.* **2018-Decem**, 527–538 (2018).
- 654 40. Shimura, K., Li, J. & Fukumoto, F. HFT-CNN: Learning Hierarchical Category Structure  
655 for Multi-label Short Text Categorization. 811–816 (2019) doi:10.18653/v1/d18-1093.
- 656 41. Akiba, T., Sano, S., Yanase, T., Ohta, T. & Koyama, M. Optuna: A Next-generation  
657 Hyperparameter Optimization Framework. *Proc. ACM SIGKDD Int. Conf. Knowl. Discov.*  
658 *Data Min.* 2623–2631 (2019).

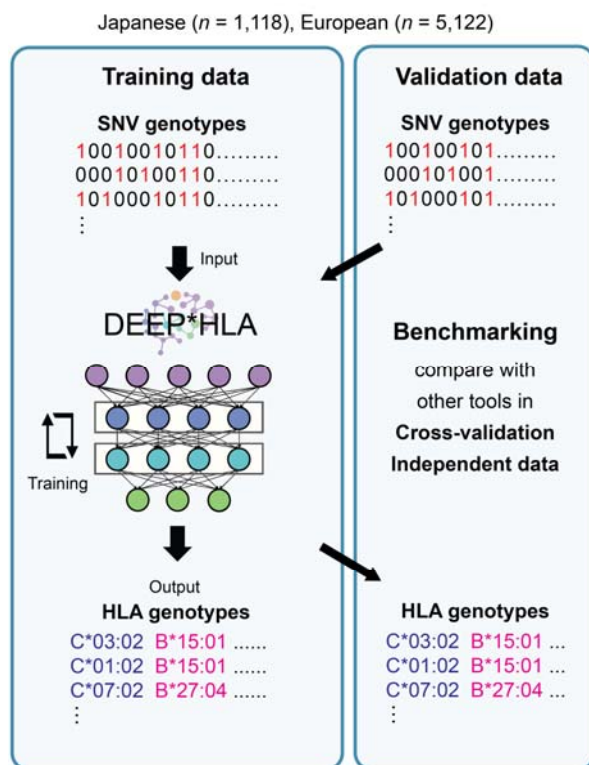
- 659 42. Zheng, X. *et al.* HIBAG - HLA genotype imputation with attribute bagging.  
660 *Pharmacogenomics J.* **14**, 192–200 (2014).
- 661 43. Nagai, A. *et al.* Overview of the BioBank Japan Project: Study design and profile. *J.*  
662 *Epidemiol.* **27**, S2–S8 (2017).
- 663 44. Hirata, M. *et al.* Cross-sectional analysis of BioBank Japan clinical data: A large cohort of  
664 200,000 patients with 47 common diseases. *J. Epidemiol.* **27**, S9–S21 (2017).
- 665 45. Kanai, M. *et al.* Genetic analysis of quantitative traits in the Japanese population links cell  
666 types to complex human diseases. *Nat. Genet.* **50**, 390–400 (2018).
- 667 46. Sudlow, C. *et al.* UK Biobank: An Open Access Resource for Identifying the Causes of a  
668 Wide Range of Complex Diseases of Middle and Old Age. *PLoS Med.* **12**, 1–10 (2015).
- 669 47. Bycroft, C. *et al.* The UK Biobank resource with deep phenotyping and genomic data.  
670 *Nature* **562**, 203–209 (2018).

671 **Figure Legends**

672

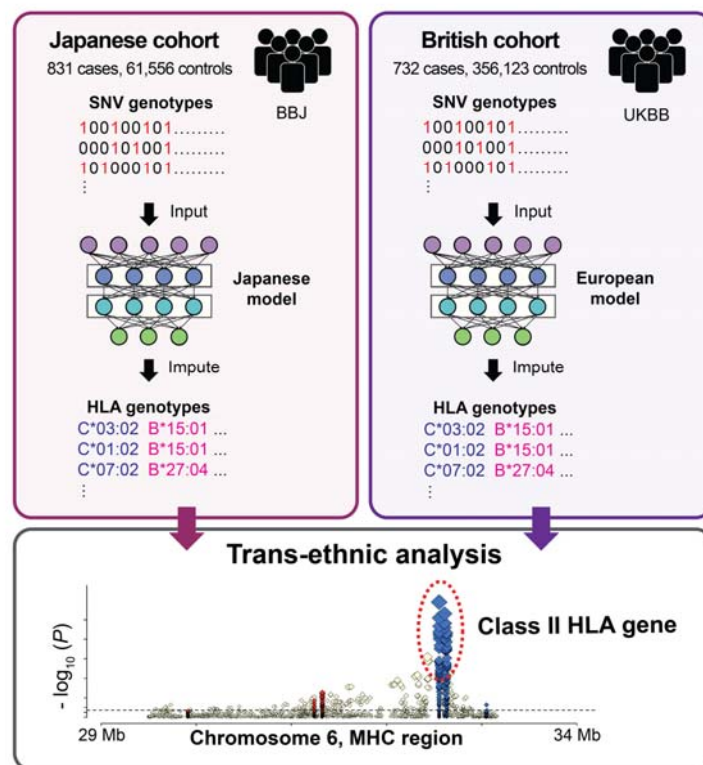
673 **Figure 1. An overview of the study**

**a Constructing models with HLA references**



674

**b MHC fine-mapping in T1D GWAS data of biobanks**



675 (a) Our method, DEEP\*HLA, is a deep learning architecture that takes an input of genotypes of

676 SNVs and outputs the genotype dosages of HLA genes. To train a model and benchmark its

677 performance, we used Japanese and European HLA reference panels respectively, and

678 evaluated its accuracies in cross-validation with compared to other tools. In the Japanese panel,

679 we also evaluated its accuracy by applying the trained model to the independent Japanese HLA

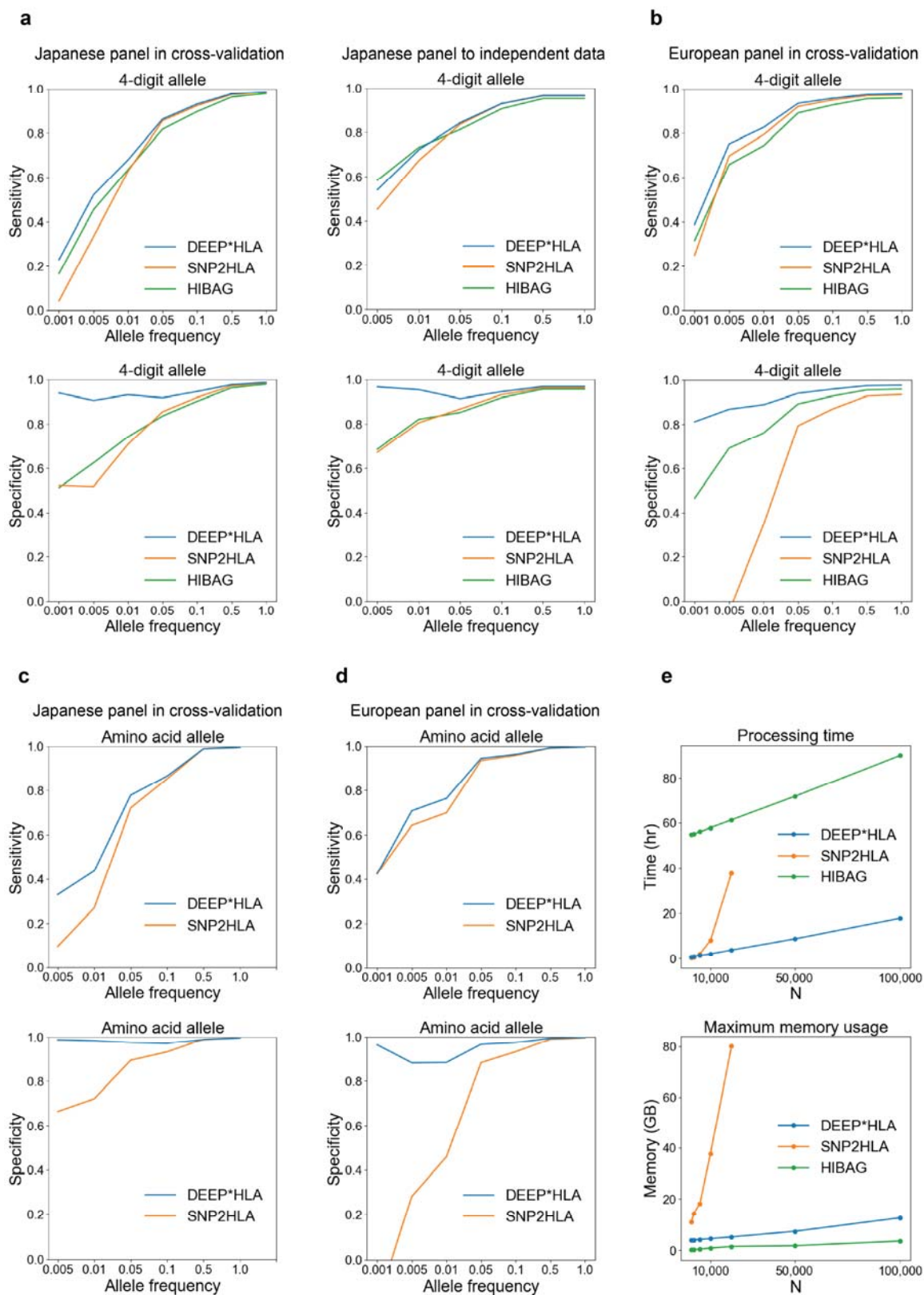
680 data. (b) We conducted trans-ethnic MHC fine-mapping in T1D GWAS data of BBJ and UKBB.

681 We performed HLA imputation for the Japanese cohort from BBJ and the British cohort from

682 UKBB using the models specific for individual populations, respectively. We integrated the

683 individual results of imputed genotypes and performed trans-ethnic association analysis.

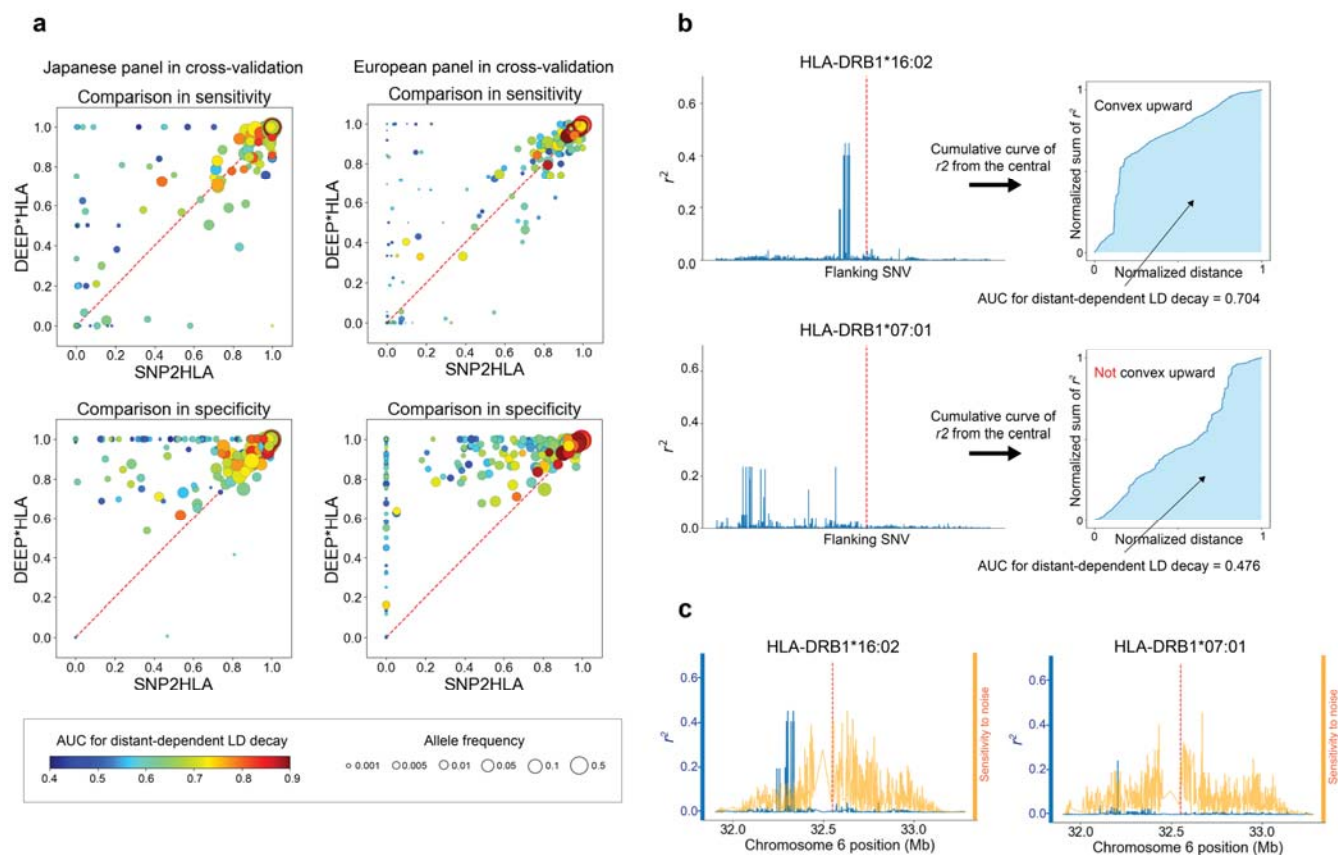
684 **Figure 2. Performance evaluations of HLA imputation methods**



685

686 **(a-d)** Sensitivity (upper) and specificity (lower) for the 4-digit alleles **(a, b)** and the amino acid  
687 polymorphisms **(c, d)** evaluated in our Japanese reference panel **(a, c)** and T1DGC reference  
688 panel **(b, d)**. For each metrics, those for alleles of which frequency is less than a value on the  
689 horizontal axis are shown on the vertical axis. As a whole, DEEP\*HLA outperformed other  
690 methods especially in specificity and imputing infrequent alleles. **(e)** Processing time (upper)  
691 and maximum memory usage (lower) evaluated on imputing the BBJ samples using the  
692 Japanese panel. DEEP\*HLA imputed by far the fastest in total processing time as the sample  
693 size increased. All methods exhibited maximum memory usage scaling roughly linearly with  
694 sample size. SNP2HLA did not work within 100 GB in our machine for the sample size of more  
695 than 20,000.

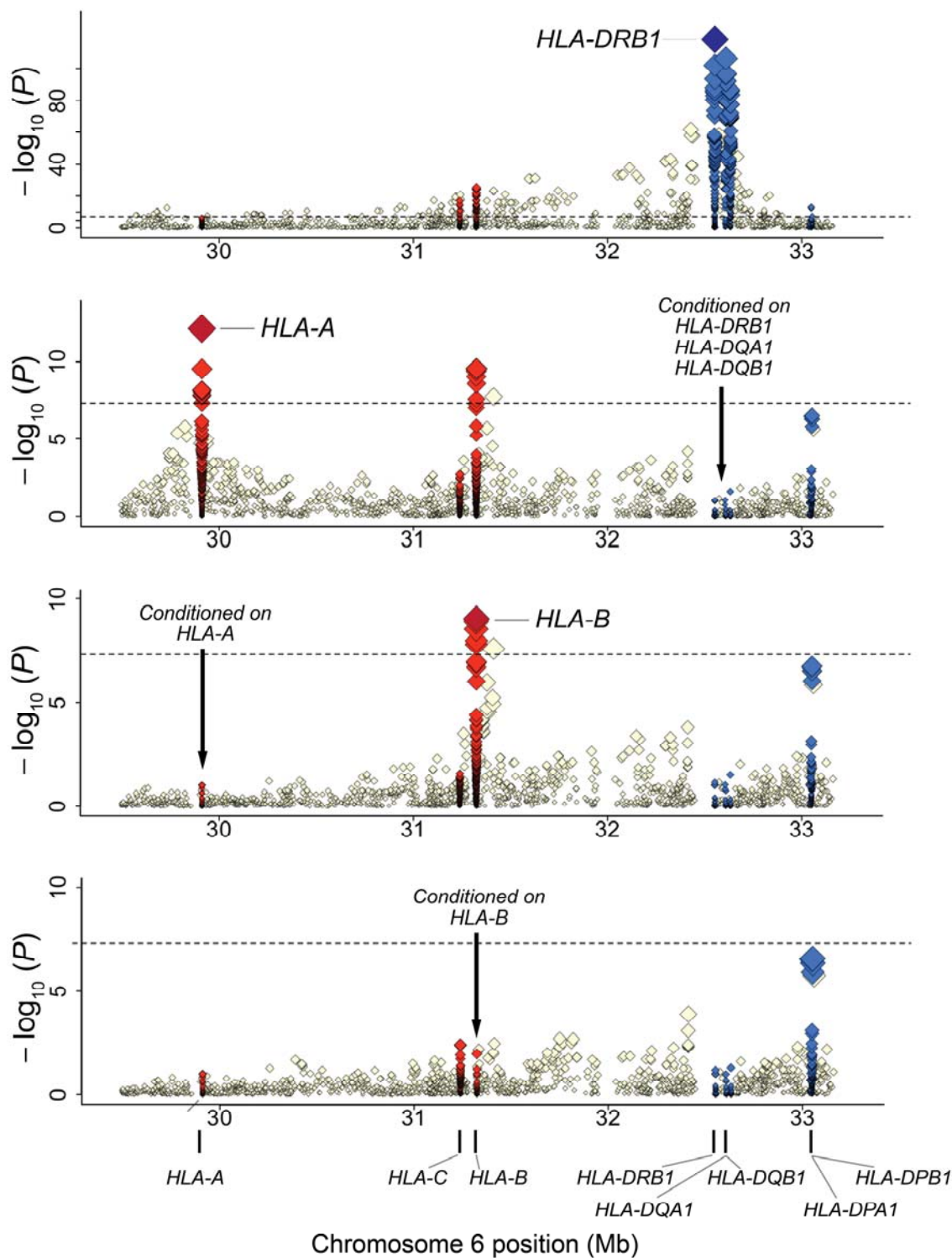
696 **Figure 3. Comparison between DEEP\*HLA and SNP2HLA displayed with allele**  
 697 **frequencies and AUC for distance-dependent LD decay**



698  
 699 **(a)** Comparisons of imputation accuracy between DEEP\*HLA and SNP2HLA in sensitivity  
 700 (upper) and specificity (lower) for 4-digit allele imputation for cross-validation on the Japanese  
 701 panel (left) and T1DGC panels (right). Each dot corresponds to one allele, displayed with allele  
 702 frequencies (size) and AUC for distance-dependent LD decay (color). Those of which  
 703 specificities were less than 0 are shown with converted to 0 for visibility. Performance of  
 704 SNP2HLA was limited when imputing the alleles with low frequency and low AUC, DEEP\*HLA  
 705 was relatively accurate even for the less frequent alleles regardless of the AUC. **(b)** Example  
 706 illustrations of AUC for distance-dependent LD decay. The left figures illustrate  $r^2$  of LD between  
 707 an HLA allele (red dash line in the central) and flanking SNVs. HLA-DRB1\*16:02 has strong LD

708 in close positions and weaker in the distance; and cumulative curve of  $r^2$  of bilateral SNVs  
709 becomes convex upward; and the AUC becomes bigger. In contrast, HLA-DRB1\*07:01 has  
710 moderate LD in distant or sparse positions; and the curve does not become convex upward;  
711 and the AUC becomes smaller. (c) Comparison between  $r^2$  (blue line) and sensitivity maps of  
712 DEEP\*HLA (orange line) for example alleles (red dash line in the central). The sensitivities are  
713 normalized for visibility. In both examples, DEEP\*HLA reacted to noises across an extensive  
714 area regardless of LD.

715 **Figure 4. Trans-ethnic association plots of the HLA variants with T1D in the MHC region.**



716

717

718 Diamonds represent  $-\log_{10}$  ( $P$  values) for the tested HLA variants, including SNPs, classical  
719 alleles and amino acid polymorphisms of the HLA genes. The dashed black horizontal lines  
720 represent the genome-wide significance threshold of  $P = 5.0 \times 10^{-8}$ . The physical positions of the  
721 HLA genes on chromosome 6 are shown at the bottom. **(a–e)** Each panel shows the  
722 association plot in the process of stepwise conditional regression analysis: nominal results. **(a)**  
723 Results conditioned on *HLA-DRB1*, *HLA-DQA1*, and *HLA-DRB1*. **(b)** Results conditioned on  
724 *HLA-DRB1*, *HLA-DQA1*, *HLA-DRB1*, and *HLA-A*. **(c)** Results conditioned on *HLA-DRB1*,  
725 *HLA-DQA1*, *HLA-DRB1*, *HLA-A*, and *HLA-B*. **(d)** Our study identified independent contribution  
726 of multiple HLA class I and class II genes to T1D risk in a trans-ethnic cohort, of which the  
727 impacts of class II HLA genes was more evident. Detailed association results are available in  
728 **Supplementary Table 4.**

729 **Tables 1. Associations of the HLA variants with T1D risk identified through the**  
 730 **trans-ethnic fine-mapping study.**

HLA variant	Frequency (BBJ)		Frequency (UKBB)		OR (95% CI)		P†	
	Case n = 831	Control n = 61,556	Case n = 732	Control n = 356,123	BBJ	UKBB	BBJ	UKBB
HLA-DRβ1 amino acid position 71								
Alanine	0.10	0.18	0.04	0.15	0.85 (0.66-1.10)	1.34 (0.89-1.99)	0.23	0.16
Arginine	0.82	0.73	0.33	0.45	(reference)			
Glutamic acid	0.073	0.074	0.083	0.12	1.26 (0.89-1.77)	0.72 (0.56-0.93)	0.019	0.0013
Lysine	0.0096	0.011	0.54	0.28	1.31 (0.71-2.24)	2.09 (1.75-2.50)	0.035	4.2 × 10 <sup>-16</sup>
HLA-DQβ1 amino acid position 185								
Isoleucine	0.39	0.57	0.68	0.83	2.74 (2.21-3.40)	4.12 (3.45-4.93)	3.5 × 10 <sup>-20</sup>	3.8 × 10 <sup>-54</sup>
Threonine	0.61	0.43	0.32	0.17	(reference)			
HLA-DQβ1 amino acid position 30								
Histidine	0.16	0.19	0.18	0.23	1.36 (0.97-1.93)	4.13 (2.86-5.95)	0.0078	3.2 × 10 <sup>-14</sup>
Serine	0.0042	0.0038	0.34	0.25	inf	3.78 (2.51-5.81)	0.079	5.3 × 10 <sup>-10</sup>
Tyrosine	0.83	0.80	0.48	0.52	(reference)			
HLA-DRβ1 amino acid position 74								
Alanine	0.56	0.59	0.59	0.65	(reference)			
Arginine	0.0018	0.00088	0.28	0.15	0 (0-0.045)	0.65 (0.42-0.97)	0.08	0.0039
Glutamic acid	0.32	0.27	0.021	0.036	0.77 (0.64-0.93)	0.57 (0.38-0.82)	0.00065	0.0004
Glutamine	0.0024	0.0030	0.0795	0.15	0 (0-0.0029)	0.31 (0.21-0.45)	0.079	5.3 × 10 <sup>-10</sup>
Leucine	0.12	0.14	0.023	0.023	0.97 (0.81-1.16)	2.19 (0.84-4.84)	0.074	0.0079
HLA-DQβ1 amino acid position 70								
Arginine	0.60	0.62	0.79	0.63	(reference)			
Glutamic acid	0.26	0.17	0.020	0.020	0.73 (0.59-0.9)	0.27 (0.11-0.72)	0.00020	0.00057
Glycine	0.14	0.20	0.19	0.35	0.95 (0.72-1.25)	0.50 (0.36-0.69)	0.073	2.9 × 10 <sup>-5</sup>
HLA-A amino acid position 62								
Arginine	0.19	0.20	0.06	0.09	1.25 (1.05-1.49)	0.93 (0.74-1.15)	0.0012	0.052
Glutamic acid	0.39	0.37	0.09	0.09	1.40 (1.21-1.63)	1.33 (1.10-1.59)	9.2 × 10 <sup>-6</sup>	0.0003
Glutamine	0.15	0.19	0.46	0.49	(reference)			
Glycine	0.26	0.24	0.33	0.29	1.44 (1.23-1.68)	1.27 (1.12-1.44)	6.6 × 10 <sup>-6</sup>	1.5 × 10 <sup>-4</sup>
Leucine	0	0	0.055	0.044	-	2.01 (1.57-2.55)	1.5 × 10 <sup>-12</sup>	1.8 × 10 <sup>-8</sup>
HLA-B*54:01	0.14	0.073	0	0	1.78 (1.51-2.08)	-	-	-

HLA, human leucocyte antigen; OR, odds ratio; 95% CI, 95% confidence interval.

†Obtained from the multivariate regression model that included all the variants listed here.